

ROBUST PERFORMANCE IN BIOPHYSICAL NETWORKS

Francis J. Doyle III ^{*,1} Jörg Stelling ^{**}

** Department of Chemical Engineering, University of California, Santa Barbara, CA, 93106, USA*

*** Institute of Computational Science, ETH, 8092 Zürich, Switzerland*

Abstract: Robust performance, the attainment of a specified response under uncertainty, is a well studied problem in control engineering. In the field of systems biology, related problems are emerging from the quantitative analysis of complex biophysical networks. In this paper, connections are made between the robust performance questions in biology and engineering. Two examples are used to illustrate these ideas: (i) a signal transduction network, and (ii) the gene network responsible for circadian oscillations. *Copyright ©2005 IFAC*

Keywords: robustness analysis, systems biology, robust performance, circadian rhythm, signal transduction

1. INTRODUCTION

In biology, as in engineering, robust performance refers to the attainment of a particular behavior or response in the presence of uncertainty. This appears to be a ubiquitous property of biological processes that are subject to constant uncertainty in the form of stochastic phenomena (McAdams and Arkin, 1999), fluctuating environment, and genetic variation (for a recent review on robustness in cellular functions, see (Stelling *et al.*, 2004b)). Biology has adapted a number of approaches for coping with these sources of uncertainty that include: redundancy, feedback control, modularity, and hierarchies and protocols. The robustness problems in systems biology have only begun to yield in recent years to formal quantitative analyses, owing largely to their nonlinear (and nonstationary) nature. As with engineering

systems, robust performance requires the precise specification of both a performance metric, and the type/size of uncertainty. When both of these elements are specified, it may be possible to analyze biological systems with the engineering tools, as will be shown in this paper. It is important to note that the performance metric is often difficult to define precisely in biology, as this is an implicit element of an evolved entity.

2. ROBUST PERFORMANCE ANALYSIS OF SIGNAL TRANSDUCTION

2.1 Biological Problem

In signal transduction, a receptor signal is “processed” in a cascaded pathway to yield a cellular response. In the example considered in this paper, the “processing” consists of a sequence of kinase and phosphatase mediated reaction steps consisting of phosphorylation and dephosphorylation steps, respectively. The key performance attributes of such a signaling system are (Heinrich

¹ Partially supported by the Institute for Collaborative Biotechnologies through grant DAAD19-03-D-0004 from the U.S. Army Research Office, and the DARPA BioCOMP program

et al., 2002): (i) speed at which signal arrives to destination, (ii) duration of signal, and (iii) strength of signal. As will be shown in this section, translation of these criteria into formal control-like specifications can be done, but only as an approximation since the formulation is set up in the frequency domain and these specifications are in the time domain.

In order to formulate such a problem in the classical robust control analysis framework, a simple model is utilized from the literature (Heinrich *et al.*, 2002). Under conditions of weak activation (low degree of phosphorylation), the individual steps in the cascade obey linear dynamics:

$$\frac{dX_i}{dt} = \alpha_i X_{i-1} - \beta_i X_i \quad (1)$$

where α_i is a pseudo first order rate constant for phosphorylation, β_i is the rate constant for dephosphorylation, and X_i is the phosphorylated form of the kinase (i). For this study, we consider the fourth order cascade detailed in the paper. In that paper, it is assumed that the receptor inactivation is approximated as a simple exponential decay, with time constant λ . In that case, one can combine the stage expressions (Equation 1) with a simple expression for the initial receptor effect to yield the overall cellular response ($Y(s)$) as the step response of the following transfer function:

$$Y(s) = \left(\frac{s}{\frac{1}{\lambda}s + 1} \right) \left(\frac{\alpha^4}{(s + \beta)^4} \right) R(s) \quad (2)$$

One simplifying assumption invoked above is that the rate constants are equal for each stage of the cascade.

In this special case (weakly activated pathways), one can actually derive explicit expressions for the various performance metrics that were specified at the beginning of this section (see derivations in (Heinrich *et al.*, 2002)). For example, the signaling time through the entire pathway is given by:

$$\tau = \frac{1}{\lambda} + \sum_{j=1}^n \frac{1}{\beta_j} \quad (3)$$

and the signal duration can be determined as:

$$\theta = \sqrt{\left(\frac{1}{\lambda^2} + \sum_{j=1}^n \frac{1}{\beta_j^2} \right)} \quad (4)$$

It is noteworthy that each of these metrics are independent of the kinase rate constants (α_i). Finally, the signal amplitude is given by:

$$S = \frac{S_0 \sum_{k=1}^n \frac{\alpha_k}{\beta_k}}{\sqrt{\left(1 + \lambda^2 \sum_{j=1}^n \frac{1}{\beta_j^2} \right)}} \quad (5)$$

From Eqs. 3-5, one can easily derive analytical expressions for signaling performance depending

on α and β , and use these to assess the results from analysis in the frequency domain.

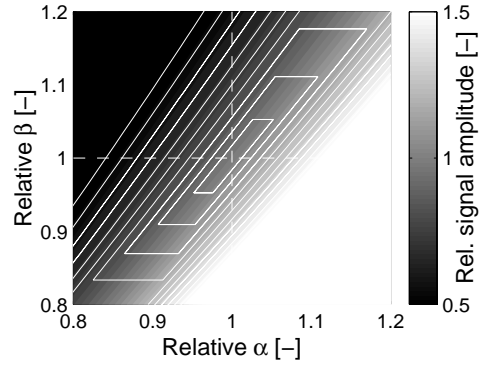


Fig. 1. Performance of a weakly activated 4-stage kinase cascade ($\alpha_j = 1.0$, $\beta_j = 0.6$ (dashed lines), $\lambda = 10.0$). Relative signal amplitude S_{rel} (gray level), and performance defined by $\pm 5\% \dots 50\%$ S_{rel} and θ_{rel} (solid lines).

For instance, in Figure 1 we assumed that a four-stage cascade should simultaneously obey bounds on the relative signal duration θ_{rel} and amplitude S_{rel} with respect to the nominal values for the reference parameter set. With these performance specifications, the system is most robust to perturbations along the diagonal in parameter space, but most sensitive to orthogonal disturbances. Notably, this is a structural feature of the system (with a nonlinear relationship between norm of the parametric perturbation and performance metric), which should be recovered by robustness analysis.

2.2 Structured Singular Value

In control engineering, a standard tool for robustness analysis is the structured singular value (SSV), which allows one to determine whether a particular dynamical system, subject to a specified (structured) uncertainty, is able to remain stable or to achieve a particular performance metric (see, for example, (Skogestad and Postlethwaite, 1996)). The two problems are known, respectively, as *robust stability* and *robust performance*, and there are standard software packages available to facilitate this computation (*e.g.*, (Balas *et al.*, 1995)). The key idea is to transform the perturbed system into a new closed-loop operator, and then to test the stability of that operator. The basic idea is illustrated in Figure 2 where the M operator denotes a nominal process system, and the Δ operator denotes the uncertainty in the system. Stability of the depicted system is equivalent to robust stability of the original problem, and if one closes a feedback loop between suitably transformed input and output signals, one obtains an operator whose stability

characteristics coincide with the attainment of robust performance in the original problem.

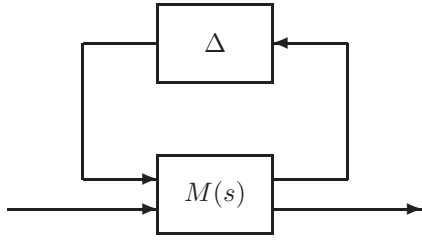


Fig. 2. Standard M- Δ Diagram for Robustness Analysis

The condition for internal stability of the M- Δ structure in Figure 2 is

$$\sup_{\omega} \mu_{\Delta}(M(j\omega)) \leq 1 \quad (6)$$

where $\mu_{\Delta}(M)$ is the structured singular value. Tight bounds on $\mu_{\Delta}(M)$ can be obtained using appropriate D-scaling matrices in the relation

$$\mu_{\Delta}(M) \leq \inf_D \bar{\sigma}(DM D^{-1}) \quad (7)$$

where $\bar{\sigma}$ denotes the maximum singular value. The upper bound on $\mu_{\Delta}(M)$ in Eq. 7 can be reformulated as a convex optimization problem to find the global minimum. MATLAB's μ -Analysis and Synthesis Toolbox (Balas *et al.*, 1995) provides the utilities required to execute this computation. Note, however, that extensions for time-varying and nonlinear uncertainty (Doyle III *et al.*, 1989) are necessary before employing the SSV analysis on nonlinear systems.

2.3 Analysis of Protein Kinase Cascade

The preceding structured singular value (SSV) analysis was applied to the kinase cascade problem. A multiplicative uncertainty was introduced for both the α and β parameters, and the impact on a performance metric was evaluated. The uncertainty was characterized as follows:

$$\alpha = \tilde{\alpha} \cdot (1 + r_{\alpha} \Delta_{\alpha}) \quad (8)$$

$$\beta = \tilde{\beta} \cdot (1 + r_{\beta} \Delta_{\beta}) \quad (9)$$

where r denotes the relative uncertainty in the coefficient, Δ denotes a scaled ($\|\Delta\| \leq 1$) uncertainty operator, and the tilde denotes a nominal value for the coefficient. The structured *parametric uncertainty* is the specific type of uncertainty considered in this case.

Algebraic manipulations yield the following representation for the uncertain transfer function from receptor to cell function:

$$\begin{aligned} \frac{Y}{R} &= \left(\frac{s}{\frac{1}{\lambda}s + 1} \right) \left(\frac{\alpha^4}{(s + \beta)^4} \right) \\ &= \left(\frac{s}{\frac{1}{\lambda}s + 1} \right) \left(\frac{\tilde{\alpha}^4}{(s + \tilde{\beta})^4} \right) \cdot \frac{(1 + r_{\alpha} \Delta_{\alpha})^4}{1 + \frac{r_{\beta} \tilde{\beta}}{s + \tilde{\beta}} \Delta_{\beta}} \quad (10) \end{aligned}$$

These manipulations were carried out for the fourth order cascade of kinase operations. Using loop algebra, this expression can be used to formulate the corresponding M- Δ block diagram.

In order to specify a performance metric, a nominal response of the operator was selected, and a performance weight was designed to yield a small margin between an actual (uncertain) response and the desired response. It should be noted that some conservatism is inevitable here, as one is translating time domain performance criteria into the frequency domain. A tracking error was introduced (difference between actual cellular response and the nominal response) and this was weighted by the filter:

$$W_e(s) = \frac{(s + b)^2}{c(s + a)} \quad (11)$$

where a , b , and c are adjustable coefficients. In this work, they were selected as (0.001, 0.2, 0.3).

Structured singular analysis was carried out for several of the examples in the original reference (Heinrich *et al.*, 2002). In the first case, the parameter set was selected to be ($\beta = 0.6, \alpha = 1.0, \lambda = 10$). The corresponding weighted performance transfer function and time domain responses are depicted in Figure 3A for a choice of relative error (both in α and β) of 4.8%. Structured singular value computations confirm that the system is robustly stable for perturbations up to magnitude $r = 0.048$. Consistent with the analytic results in the time domain, the perturbations with opposite signs (α versus β) yield the largest deviation in both signal duration and amplitude.

A second set of parameters was investigated ($\beta = 1.1, \alpha = 1.0, \lambda = 1.0$), and it was found that the original 4.8% perturbation has a very small impact on the system performance. This is confirmed with formal structured singular value computation, which yields a maximum perturbation magnitude of 0.162, indicating that nearly four times the magnitude of perturbation is acceptable for this nominal parameter set (confirmed in Figure 3B). Once again, the direction of the perturbation is important, and the results are consistent with the previous case.

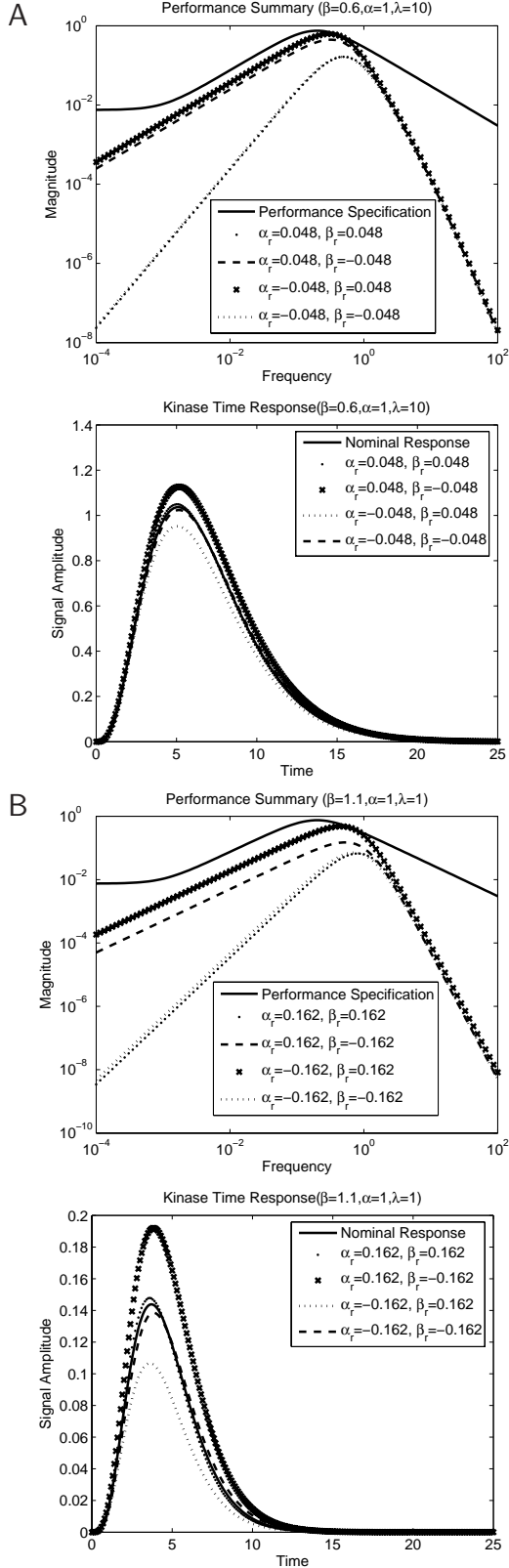


Fig. 3. Performance Summary for kinase cascade with parameter sets $\alpha = 1.0$, $\beta = 0.6$, $\lambda = 10.0$ (A) / $\lambda = 1.0$ (B), and 4.8% (A) / 16.2% (B) multiplicative parameter uncertainty. Nominal performance bound and 4 permutations of maximal uncertain values with corresponding transfer function magnitude in frequency domain (top plots) and time domain response to unit step input (bottom plots).

3. ROBUST PERFORMANCE ANALYSIS OF CIRCADIAN RHYTHM

3.1 Biological Problem

Genetic oscillators, in particular those generating 24-hour (circadian) rhythms, have emerged as model systems for studying the robustness of cellular dynamics. In reality, the evolutionary conserved period generator displays a complex architecture with several negative and positive feedback loops controlling gene expression. This complexity most likely results from the need for robust performance (Stelling *et al.*, 2004a). Performance metrics for this system, however, are not easily derived because it is largely unclear, which features of the autonomous oscillator (in constant darkness), or of its synchronization with external rhythms by light (entrainment) are most crucial for the physiological function of the system.

Here, we started analyzing performance metrics and robustness of the entrained system by using a simple ODE model for the circadian oscillator in the fruit fly *Drosophila* (Tyson *et al.*, 1999). The reduced (via steady-state approximation) 2-state model is given by

$$\frac{dM}{dt} = \frac{v_m}{1 + (P_t(1-q)/2P_{crit})^2} - k_m M \quad (12)$$

$$\frac{dP_t}{dt} = v_P M - \frac{k_{p1} P_t q + k_{p2} P_t}{J_p + P_t} - k_{p3} P_t \quad (13)$$

$$\text{with } q = \frac{2}{1 + \sqrt{1 + 8K_{eq} P_t}}, \quad (14)$$

and M and P_t being the total mRNA and protein concentrations of a single regulator, respectively. Altogether, nine parameters describe kinetic properties of the biochemical reactions considered in the model. A unit square-wave forcing signal $u(t)$ with period τ_F was used for the entrainment. By replacing the equilibrium constant in Eq. 14 with

$$K'_{eq}(t) = [1 - \alpha u(t)] K_{eq}, \quad (15)$$

α was an adjustable parameter for the strength of the entraining signal (Tyson *et al.*, 1999). Solutions for the ODE system were obtained by numerical integration with MATLAB's *ode15s* solver (The Mathworks Inc., Natick, MA).

3.2 Performance metrics for entrainment

Performance metrics for biological systems have to be derived from – usually incompletely characterized – physiological functions the underlying control circuits were presumably optimized for. For the circadian oscillator, biologically plausible performance criteria could include

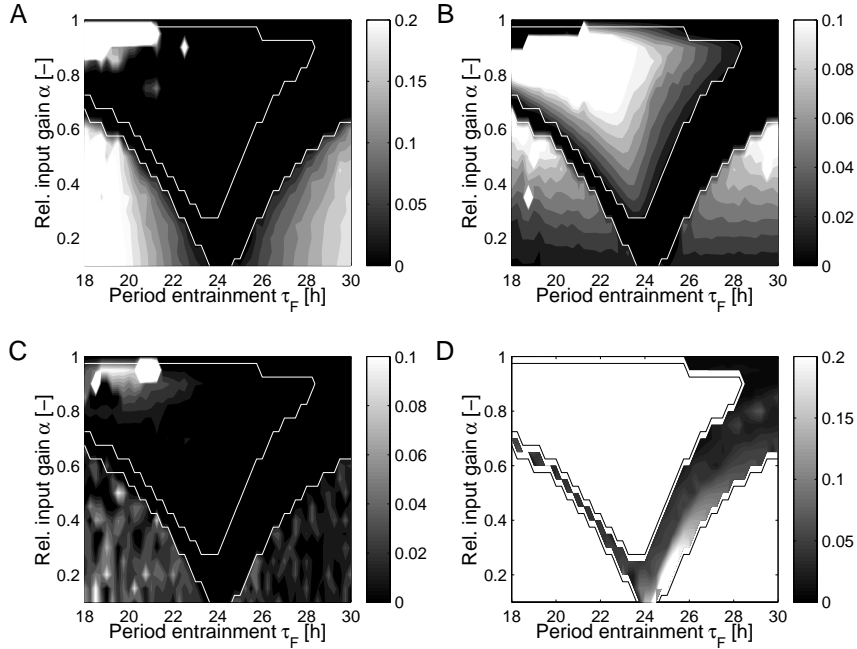


Fig. 5. Systematic assessment of performance criteria for entrainment. (A) Normalized deviation of the average oscillator period, i.e. $|1 - \bar{\tau}|$, (B) Standard deviation of the normalized period, σ_τ , (C) Persistent phase difference ($\phi_F = +\tau_F/2$), φ , and (D) Average time-constant for re-synchronization, $t_{1/2}$. White lines demarcate the region of perfect entrainment as defined in the text.

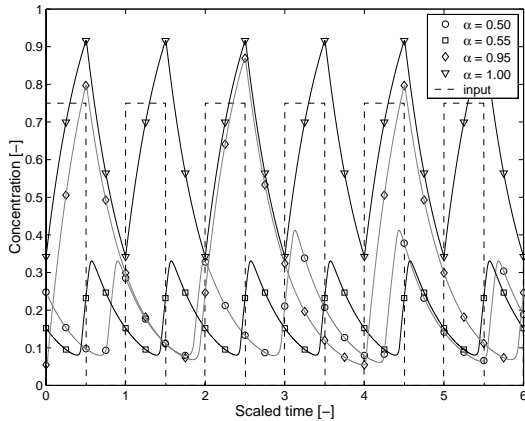


Fig. 4. Entrained oscillations in $M(t)$ for $\tau_F = 22h$ and varying α . Perfect (black) and imperfect (gray) entrainment by light input (dashed).

- (1) robust perfect entrainment to light inputs of constant period and amplitude, and
- (2) rapid adaptation to phase shifts in the input to minimize phenomena such as "jet-lag".

To analyze the circadian oscillator according to these criteria, period (τ_F) and coupling strength (α) of the forcing signal were varied systematically, and the resulting stable oscillations were recorded. Figure 4 shows representative trajectories of the mRNA concentration $M(t)$ for fixed τ_F and different values of α , illustrating the complex dynamics of the forced system. For instance, perfect entrainment, i.e. regular oscillations with period τ_F , was obtained only for maximal ($\alpha = 1.0$) and some intermediary ($\alpha = 0.55$) coupling val-

ues. Slightly different parameters induced period doubling ($\alpha = 0.95$) and irregular oscillations with an average period of τ_F ($\alpha = 0.5$), respectively.

Assessing the precision of entrainment, hence, required at least two performance specifications regarding the average period length, $\bar{\tau}$, and its variability (standard deviation) σ_τ . In brief, the period of the entrained system $\tau(t)$ was derived by detection of maxima in $M(t)$ to calculate $\bar{\tau}$ and σ_τ from a normalized $\tau'(t) = \tau(t)/\tau_F$. Both measures were then analyzed in the $\tau_F \times \alpha$ plane to characterize the oscillator's performance with respect to a constant entraining signal (Figure 5A,B). We considered the circadian clock as perfectly entrained whenever $|1 - \bar{\tau}| \leq 0.01$ and $\sigma_\tau \leq 0.01$. In general, as would be expected, closer coupling of the oscillator with the input signal, and an input period near the free-running period of the circadian system ($24.2h$) favor entrainment. The data in Figure 5B, however, indicates that, in contrast to a previous analysis (Tyson *et al.*, 1999), the simplified model has only a small region of perfect entrainment because irregular oscillations arise at average values of α . This underlines the need for exact specification of performance criteria, and supports the view that the oscillator's additional complexity may provide robust performance under input uncertainties (Stelling *et al.*, 2004a).

Speed and accuracy of tracking phase shifts in the forcing signal that occur, for instance, when traveling across time-zones, constitutes a second possible performance criterion for the circadian

clock. Phase shifts ϕ_F in $u(t)$ with $-\tau_F/2 \leq \phi_F \leq +\tau_F/2$ were therefore applied to the (partially) entrained system, and the transient dynamics were analyzed. Typically, for perfectly entrained conditions as defined above, the system rapidly adapted to the new phase; only minor dependencies on ϕ_F were observed (Figure 6).

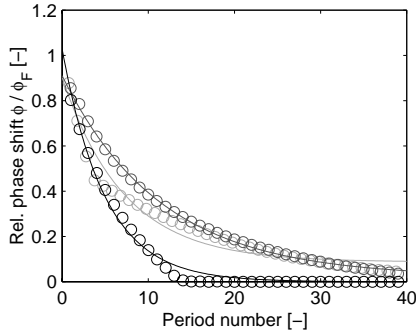


Fig. 6. Re-synchronization of the circadian oscillator after a $\phi_F = +\tau_F/2$ phase shift in the input with $\tau_F = 25$ h, $\alpha = 0.2 \dots 0.4$ (light gray to black). Phase differences between maxima of $M(t)$ (symbols) normalized by ϕ_F , and approximations (Eq. 16, lines).

To quantitatively characterize re-synchronization of the clock, we established an approximation for the time-course of the phase difference $\phi_{\tau_F, \alpha}(t)$, exploiting the similarity to first-order decay processes when the phase shift occurs at $t = 0$:

$$\phi_{\tau_F, \alpha}(t) \approx \phi_F^{-1} k_3 (\exp(-k_1 \cdot t/\tau_F) + k_2). \quad (16)$$

Here, k_1 describes the time-constant of decaying phase differences, which can be employed to calculate a 'half-life' of the differences as $t_{1/2} = \ln(2)/k_1$. The persistent phase difference for $t \rightarrow \infty$, accordingly, is given by $\varphi = \phi_F^{-1} \cdot k_2 \cdot k_3$. Systematic analysis for these two measures, however, revealed only weak dependencies on coupling strength α and forcing period τ_F (Figure 5C,D). In future studies, hence, the precision of entrainment as a prerequisite for adaptation should move into the focus of the analysis.

4. SUMMARY

In this paper, we have drawn connections between classical engineering approaches to robust performance analysis, and the corresponding problems in systems biology. Although there are some restrictions on the class of systems that are amenable to this type of analysis, the tools allow straightforward application to problems with hundreds of states, and a comparable number of sources of structured uncertainty (e.g., parametric uncertainty). By comparison, there are recently reported specialized mathematical results that are

potentially less conservative, but are restricted to narrow classes of problems (Chaves *et al.*, 2004).

There is a clear tradeoff between performance levels and the magnitude and type of uncertainty, as was illustrated in the examples in this paper. Furthermore, as was shown in the signal transduction example, the nonlinear behavior at different operating points (parameter sets) yields different results for robust performance. The precise tradeoffs can be computed in the form of a performance curve using skewed μ (Skogestad and Postlethwaite, 1996). Such tradeoff curves would be rather valuable in the analysis of complex biological systems.

A more subtle point is worth emphasizing on the tradeoffs between performance and uncertainty in biological systems. In some cases, uncertainty may be characterizable, based on stochastic variations that are modeled, or environmental perturbations that are predictable. In other cases, the precise form of the structured uncertainty may be difficult to characterize. In general, the performance objectives employed by nature – whether on a real-time basis or on an evolutionary timescale – remain an elusive goal for scientists to determine by reverse-engineering. The performance metric may be high-dimensional, and also depend upon the boundaries drawn for analysis: for example, the goal of a single circadian gene network in a neuron is not likely to be the same as the goal of a population of 10,000 synchronized neurons in the brain.

REFERENCES

- Balas, G. J., J. C. Doyle, K. Glover, A. Packard and R. Smith (1995). *μ -Analysis and Synthesis Toolbox User's Guide*. The Mathworks. Natick, MA.
- Chaves, M., E. Sontag and R. Dinerstein (2004). Optimal Length and Signal Amplification in Weakly Activated Signal Transduction Cascades. *J. Phys. Chem.* **108**, 15311–15320.
- Doyle III, F. J., A. K. Packard and M. Morari (1989). Robust controller design for a nonlinear CSTR. *Chem. Eng. Sci.* **44**, 1929–1947.
- Heinrich, R., B.G. Neel and T.A. Rapoport (2002). Mathematical models of protein kinase signal transduction. *Mol. Cell* **9**, 957–970.
- McAdams, H. H. and A. Arkin (1999). It's a noisy business: Genetic regulation at the nanomolar scale. *Trends Genet.* **15**, 65–69.
- Skogestad, S. and I. Postlethwaite (1996). *Multivariable Feedback Control*. John Wiley & Sons, New York, NY.
- Stelling, J., E.D. Gilles and F.J. Doyle III (2004a). Robustness properties of circadian clock architectures. *Proc. Natl. Acad. Sci. USA* **101**, 13210–15.
- Stelling, J., U. Sauer, Z. Szallasi, F.J. Doyle III and J. Doyle (2004b). Robustness of cellular functions. *Cell* **118**, 675–685.
- Tyson, J.J., C.I. Hong, C.D. Thron and B. Novak (1999). A simple model of circadian rhythms based on dimerization and proteolysis of PER and TIM. *Biophys. J.* **77**, 2411–17.